

# Chapter Number: X

## Locomotion Principles of 1D Topology Pitch and Pitch-Yaw-Connecting Modular Robots

Juan Gonzalez-Gomez<sup>1</sup>, Houxiang Zhang<sup>2</sup> & Eduardo Boemo<sup>1</sup>

<sup>1</sup>*Universidad Autonoma de Madrid  
Spain*

<sup>2</sup>*University of Hamburg  
Germany*

### 1. Introduction

The last few years have witnessed an increasing interest in modular reconfigurable robotics. The applications include industrial inspection (Granosik, 2005), urban search and rescue (Zhang, 2006a), space applications (Yim, 2003) and military reconnaissance (Zong, 2006). They are also very interesting for research purposes. Modular robots are composed of some identical or similar units which can attach and detach each other and are capable of changing the configurations.

Some modular prototypes are quite famous, such as Polybot (Yim, 2000), CONRO (Castano, 2000), SuperBot (Chen, 2006) from Information Sciences Institute and Computer Science and M-TRAN robot (Kurokawa, 2003). Some common ideas of these prototypes lie in two points. Normally this kind of robots consists of many modules which are able to change the way they are connected. In further the modular approach enables robots the reconfiguration capability which is very essential in such tasks which are difficult for a fixed-shape robot. It also enables the mobile robotic system the characteristics of versatility, robustness, low-cost and fast-prototyping so that new configurations of different robots can be built fast and easily, for the exploration, testing and analysis of new ideas. More exciting advantage is that the robots have the capability of adopting different locomotion to match various tasks and suit complex environments.

Modular robots can be classified according to both the connection between the modules and the topology of its structure. One important group is the Snake robots. It includes the configurations consisting of one chain of modules (1D Topology). The locomotion is performed by means of body motions. Depending on the type of connection between the modules, there are pitch, yaw and pitch-yaw connecting snakes robots. The locomotion capabilities of the yaw family have been deeply studied (Hirose, 1993). There are also research works about the locomotion capabilities of some specific pitch-yaw modular robots. In (Chen, 2004) the rolling gaits are deeply studied and (Mori, 2002) implemented different gaits in the

ACM robot. However, the locomotion principles for the whole pitch-yaw family have not been fully studied.

In this chapter we propose a model for the locomotion of the pitch-yaw snake robots that allow them to perform five different gaits: forward and backward, side-winding, rotating, rolling and turning. The rotating gait is a new one that has not been previously achieved by other researchers, from the best of our knowledge. Each joint is controlled by means of a sinusoidal oscillator with four parameters: amplitude, frequency, phase and offset. The values of these parameters and the relations between them determine the type of gait performed and its trajectory and velocity. The locomotion in 1D and 2D for both, the pitch and pitch-yaw connecting modular robots are studied. The relationships between the oscillator parameters to achieve the different gaits are summarized in twelve locomotion principles.

Another issue are the minimal configurations (Gonzalez-Gomez, 2005) that can move both in 1D and 2D. They are novel configurations that minimize the number of modules needed to perform the locomotion. This idea is important for maximizing the number of robots in which a self-reconfigurable robot can be split without losing any locomotion capabilities. Experiments show that configurations consisting of two and three modules can move in 1D and 2D respectively. Their locomotion principles are also presented.

Four prototypes have been built: two minimal configurations and two eight-modules snakes, with both pitch and pitch-yaw connections. A series of successful tests are given to confirm the principles described above and the robot's ability. In the end of the chapter, our future work and some conclusions are given.

## 2. Classification of Modular Robots

A general classification of the different configurations of modular robots is essential for the study of their properties. One classification that has been previously proposed by the authors (Gonzalez-Gomez, 2006) is shown in Fig. 2.1. The explanation follows.

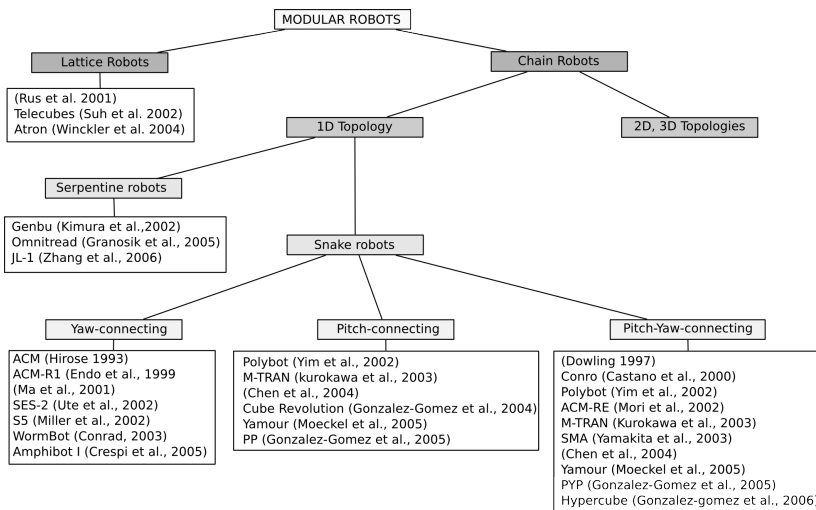


Fig 2.1. General classification of modular robots

Mark Yim established a first classification of modular robots in two groups: lattice and chain robots. The former arranges modules to conform a grid, just like atoms conforming complex 3D molecules or solids. One of the promises of this kind of robots is building solid objects, such as cups or chairs, and then rearranging the atoms to form other solids. The latter structures are composed of chains of modules. For example, the structure of a four legged robot can be thought as a robot with five chains. That means one chain acts as the main body (or the cord) and the other four chains form the legs. Chain-robots are suitable for locomotion and manipulation since the modular chains are like legs or arms. They consist of a series chain of linked modules to form snakes, worms, legs, arms or cords, even loops. The more modules are used, the more configurations are achieved.

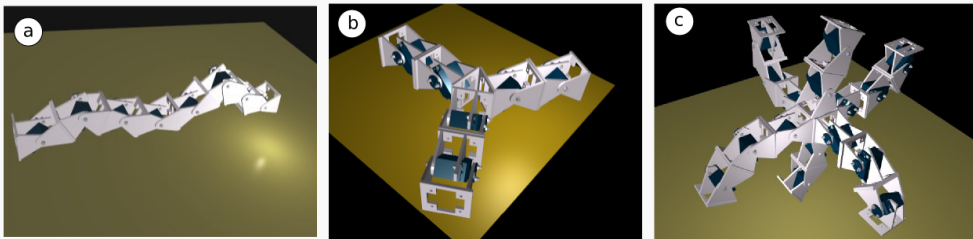


Fig 2.2. Examples of the three sub-types of chain robots. (a) 1D topology. (b) 2D topology. (c) 3D topology

Chain-robots are classified according to their topology, as shown in Fig.2.2. If the robot consists of a series chain of linked modules, the topology is called 1D chain. Two or more chains can be connected forming 2D-chain topologies like triangles, squares, stars and so on, which can be placed on a plane when they are in the home states. Finally, the chains forming a cube, pyramid, 3D star, is called as a 3D topology. In principle, 2D and 3D chain robots can move by body motions or using legs. In general, they are more stables, because they can have more points contacting with the ground.

1D-chain robots are like snake, worms, legs, arms or cords. They can change their bodies to adopt different shapes. They are suitable for going through tubes, grasping objects and moving in rough terrain. If the length is enough, they can form a loop and move like a wheel. As an example, Mark Yim (Yim, 2000) proposed the famous reconfigurable robot PolyBot which is able to optimize the way its parts are connected to fit the specific task. It adopts its shape to become a rolling type for passing over flat terrain, an earthworm type to move in narrow spaces and a spider type to stride over uncertain hilly terrain.

1D-chain robots can be grouped according to their locomotion capabilities. In (Granosik, 2005) the author proposes to divide them into serpentine and snake robots. The first group features active modules which comprises several identical similar modules with full locomotion capability. Every unit or module is an entire robot system that can perform distributed activities. Meanwhile all of them can also connect with each other by some special designed docking joints which enable the adjacent modules to adopt optimized configurations to negotiate difficult terrain or to split into several small units to perform tasks simultaneously. A sub-classification of this kind of modular robots according to their kinematics modes includes wheeled and chain-track vehicles. Robots with a wheeled and chain-track vehicle are relatively portable due to high adaptability to unstructured environments. It is noted that the first modular prototype (Hirose, 1990) with powered wheels was designed by Hirose and

Morishima, which consists of several vertical cylindrical segments. The robot looks like a train. However, with a weight of over 300 kg it is too heavy. Another mobile robot with six active segments and a head for the inspection of sewage pipes was developed in (Klaasen 1999). There are twelve wheels on each module to provide the driving force.

Another example of a serpentine robot is JL-I (Zhang, 2006b) with various moving modes. The system consists of three connected, identical modules for crossing grooves, steps, obstacles and traveling in complex environments. JL-I features three-degrees-of-freedom (DOF) active joints for changing shape and flexible docking mechanism. In order to enable highly adaptive movement, the robot's mechanical structure is employed to drive serial and parallel mechanisms to form active joints for changing shape in three dimensions (3D).

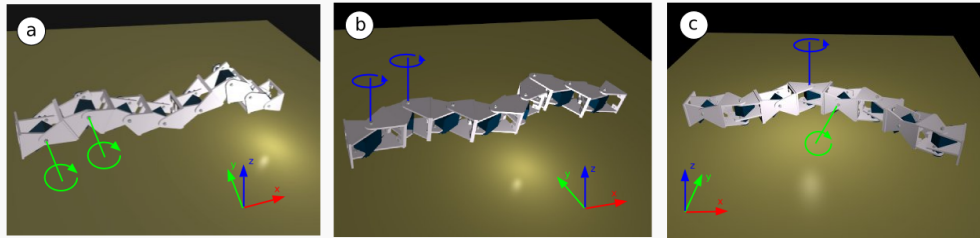


Fig 2.3. Different connections for a snake robot. (a) Pitch connecting. (b) Yaw connecting. (c) Pitch-yaw connecting.

The snake robot are only propelled by means of body motions. This group can be divided into three groups according to the connection axis between two adjacent modules: Pitch, yaw and pitch-yaw connecting snake robots. It is shown in Fig. 2.3.

The pitch-connecting robots only can move in 1D, forward or backward. Its movement can be generated by means of waves that travel the body of the robot from the tail to the head. M-TRAN (Kurokawa, 2003), Yamour (Moeckel, 2005) and Polybot (Yim, 2000) can be connected in a pitch-pitch way. The Cube robot (Gonzalez-Gomez, 2004) is another example. It is controlled by means of Field Programable Gate Arrays (FPGAs) technology that generate the body waves.

The yaw-connecting robots move like the real snakes. All the joints rotate around the yaw axis. In order to get propelled, these robots creep along a given curve path, but the body should slip in the tangential direction without any sliding in the direction normal to the body axis. A lot of researches have been done on this kind of robots. Noted that yaw-connecting robots were first studied by (Hirose, 1993) who developed the Active Cord Mechanism (ACM). Recently some new versions were developed in his group (Mori, 2002). S. Ma et al. in Japan and his Chinese colleagues at the Robotics Laboratory of Shenyang Institute of Automation also developed their own yaw-connecting robot and studied the creeping motion on a plane (Ma 2006) and on a slope (Chen, 2004). Another prototypes are SES-2 (Ute, 2002), S5 (Miller, 2002), WormBot (Conradt, 2003) and swimming Amphibot I (Crespi 2005).

The pitch-yaw-connecting modular robots have some modules that rotates around the pitch axis and others around the yaw axis. These robots have new locomotion capabilities, like side-winding, rotating and rolling. Some pitch-yaw-connecting robots have modules with two DOFs. Others have one DOF and can only be connected in a pitch-yaw way, like ACM-R3 (mori, 2002) and SMA (Yamakita, 2003).

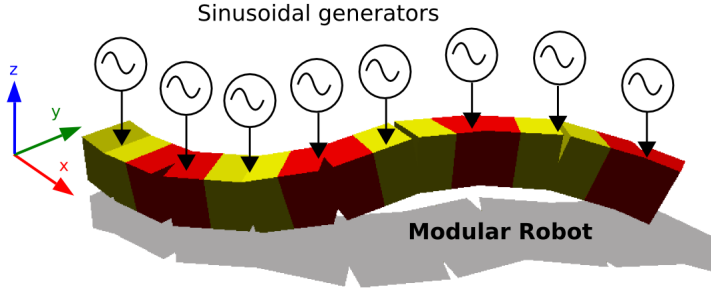


Fig 3.1. Control approach for the locomotion of the pitch and pitch-yaw connecting modular robots.

### 3. Control approach

#### 3.1 Introduction

In this section the control scheme is presented and the solution space is analyzed. Two solution sub-spaces  $H1$  and  $H2$  are proposed for the study of the locomotion principles of the pitch and pitch-yaw connecting robot group from a general point of view. These spaces are characterized by the appearance of body waves that propagate along the body axis of the robot. These waves determine the characteristics of the gaits. They will be used in the following sections to understand the locomotion principles.

#### 3.2 Sinusoidal generators

A Biologically inspired model is used to perform the locomotion. It is based on sinusoidal generators to produce rhythmic motion on the modules. These generators act like the Central Pattern Generators (CPGs) located in the spinal cord of the animals. This idea is shown in figure 3.1. There is one generator connected to each module. The bending angles of the joints are given by the equation (1). All the parameters used are listed in table 3.1.

$$\varphi_i(t) = A_i \sin\left(\frac{2\pi}{T_i} t + \phi_i\right) + O_i \quad i \in [1..M] \quad (1)$$

Symbols	Descriptions	Range
$\varphi_i(t)$	Bending angle of the module $i$	$[-90,90]$ degrees
$A_i$	Amplitude of generator $i$	$[0,90]$ degrees
$T_i(t)$	Period of generator $i$	Time units
$\phi_i(t)$	Phase of generator $i$	$(-180,180]$
$O_i$	Offset of generator $i$	$[-90,90]$ degrees
$M$	Number of modules of the robot	$M \geq 2$

Table 3.1. Parameters of the sinusoidal generators

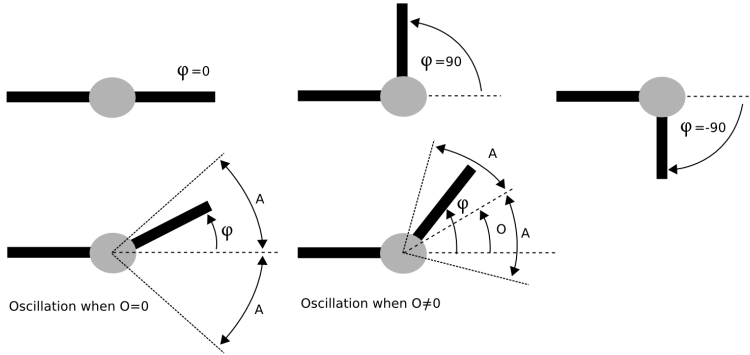


Fig 3.2. The parameters of the sinusoidal generators.

In Fig 3.2 a graphical representation of the parameters is shown. The bending angle always satisfy that  $\varphi_i \in [O_i - A_i, O_i + A_i]$ . As the maximum rotation range of the articulation is 180 degrees, the following restriction is also met  $|O_i| + A_i \leq 90$ .

### 3.3 Solution spaces

For achieving the locomotion of the robot the values of the parameters for all the generators should be found. As the robot has  $M$  modules, there are  $M$  sinusoidal generators that make them oscillate. Each generator have four independent parameters ( $A_i, T_i, \Phi_i, O_i$ ). Therefore, there are  $4M$  parameters in total and the dimension of the solution space is also  $4M$  dimensions:  $S(M) = \{\vec{v} \in \mathbb{R}^{4M} | \vec{v} = (A_1, T_1, \phi_1, O_1, \dots, A_M, T_M, \phi_M, O_M)\}$ .

The problems of finding and optimizing gaits can be tackle by means of searching techniques in the  $S(M)$  space, like genetics algorithms, simulated annealing and so on.

In order to study the locomotion principles for the whole family of pitch and pitch-yaw connecting modular robots, two new subspaces are defined:  $H1$  and  $H2$  respectively. These spaces have the advantage that the solutions do not depend on the number of modules ( $M$ ) of the robot.

### 3.4 Solution space H1

The solution subspace  $H1$  is obtained when the following assumptions are made:

- All the generators have the same amplitud ( $A$ ) and period ( $T$ )
- All the generators have no offset
- The phase difference between two consecutive generators is always the same ( $\Delta\Phi$ )
- A generator located at one of the ends of the robot is taken as a phase reference, with  $\Phi_1 = 0$

It is defined as  $H_1 = \{\vec{h} \in \mathbb{R}^3 | \vec{h} = (A, \Delta\Phi, T)\}$ . It only has three components and the solutions does not depend on the number of modules ( $M$ ). The oscillation of the joints is given by the equation (2). This space is used for studying the locomotion principles for the pitch-connecting modular robots. In Fig 3.3 a graphical representation of the controlling system using this solution is shown.

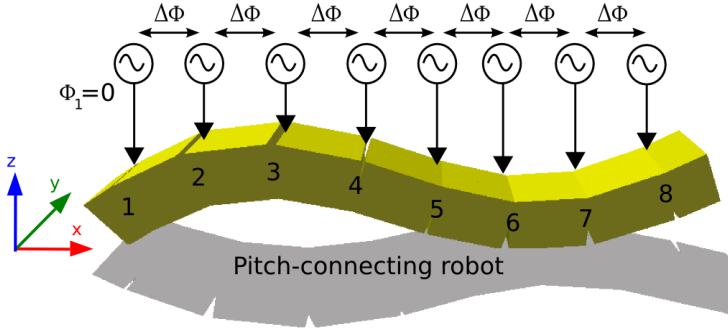


Fig 3.3. Control of a pitch-connecting modular robot using the solution space H1

$$\varphi_i(t) = A \sin\left(\frac{2\pi}{T}t + (i-1)\Delta\Phi\right) \quad i \in [1 \dots M] \quad (2)$$

$$\varphi_{v_i}(t) = A_v \sin\left(\frac{2\pi}{T}t + (i-1)\Delta\Phi_v\right) \quad i \in \left[1 \dots \frac{M}{2}\right] \quad (3)$$

$$\varphi_{H_i}(t) = A_H \sin\left(\frac{2\pi}{T}t + (i-1)\Delta\Phi_H + \Delta\Phi_{vH}\right) + O_H \quad i \in \left[1 \dots \frac{M}{2}\right] \quad (4)$$

### 3.5 Solution space H2

The solution subspace  $H2$  is obtained when the following assumptions are made:

- The modules are divided into vertical and horizontal
- All the vertical generators have the same amplitude  $A_v$
- All the horizontal generators have the same amplitude  $A_h$
- The phase difference between two consecutive vertical modules is  $\Delta\Phi_v$
- The phase difference between two consecutive horizontal modules is  $\Delta\Phi_H$
- The phase difference between the vertical and horizontal generators is  $\Delta\Phi_{vH}$
- The vertical generators have no offset
- The horizontal generators have all the same offset  $O_h$
- The first vertical generator is taken as a phase reference with  $\Phi_{v1}=0$
- All the generators have the same period  $T$

It is defined as  $H_2 = [\vec{h} \in \mathbb{R}^7 | \vec{h} = (A_v, A_H, \Delta\Phi_v, \Delta\Phi_H, \Delta\Phi_{vH}, O_H, T)]$ . It is used to study the locomotion principles of the pitch-yaw-connecting modular robots. The oscillation for both vertical and horizontal modules is given by the equations (3) and (4). A graphical representation of these generators controlling a pitch-yaw-connecting modular robots is shown in Fig 3.4.

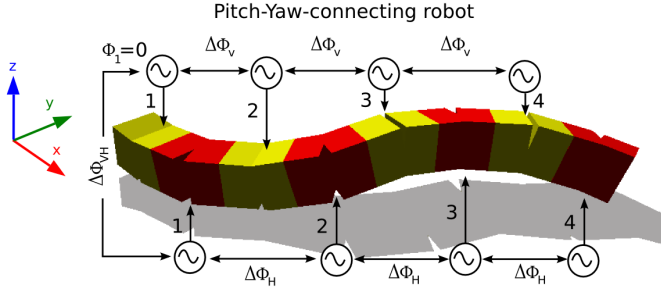


Fig. 3.4. Control of a pitch-yaw-connecting modular robot using the solution space H2

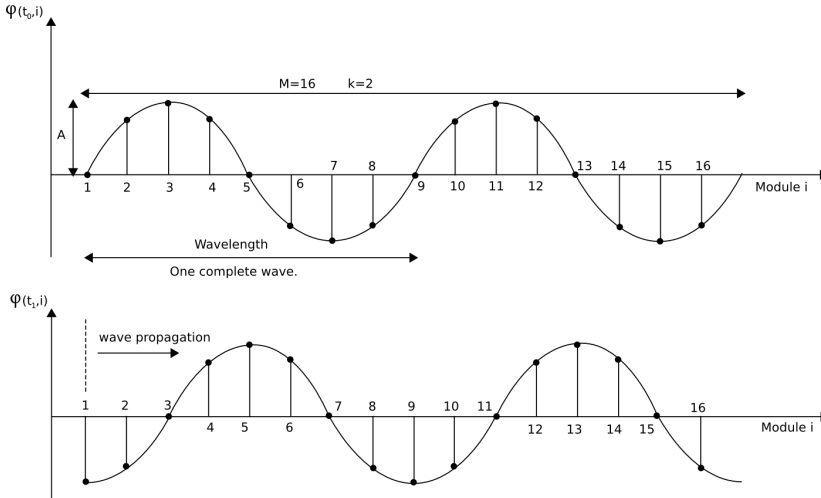


Fig 3.5. The angular wave at instants t0 and t1

### 3.6 Angular waves

One important property of the  $H1$  and  $H2$  subspaces is that the solutions can be described as angular waves  $\varphi(t, i)$  that propagate through the joints. They have an amplitude, a wavelength, a number of complete waves ( $k$  parameter) and a period. In Fig 3.5 a representation of an angular wave at two instants is shown. It has a wavelength of eight modules and  $k=2$ . It is propagating to the right.

The equation (2) can be rewritten as:

$$\varphi(t, i) = A \sin\left(\frac{2\pi t}{T} + \frac{2\pi k}{M}(i-1)\right) \quad i \in [1 \dots M] \quad (5)$$

where the parameter  $\Delta\Phi$  has been expressed as a function of  $M$  and  $k$  (equation (6)).



$$\Delta\Phi = \frac{2\pi k}{M} \quad (6)$$

The same idea is valid for the  $H2$  subspace. The equations (3) and (4) can be rewritten as (8) and (9). The subscripts  $v$  and  $h$  refer to vertical and horizontal modules respectively. Each group have their own set of parameters  $A$ ,  $k$  and  $\Delta\Phi$ . There are two angular waves, one that propagates along the vertical joints and another that does though the horizontal.

$$\varphi_v(t, i) = A_v \sin\left(\frac{2\pi t}{T} + \frac{2\pi k_v}{M/2}(i-1)\right) \quad i \in \left\{1 \dots \frac{M}{2}\right\} \quad (8)$$

$$\varphi_H(t, i) = A_H \sin\left(\frac{2\pi t}{T} + \frac{2\pi k_H}{M/2}(i-1) + \Delta\Phi_{vH}\right) + O_H \quad i \in \left\{1 \dots \frac{M}{2}\right\} \quad (9)$$

### 3.7 Body waves

The angular waves determine the shape of the robot at every instant  $t$ . Due to its propagation, there appear a body wave  $B(t, x)$  that travels along the robot. Its parameters are: the amplitude ( $A_B$ ), wavelength ( $\lambda$ ), the number of complete waves ( $k$ ) and the period ( $T$ ). In figure 3.6 a pitch-connecting robot of ten modules is shown at an instant  $t$  along with its body wave.

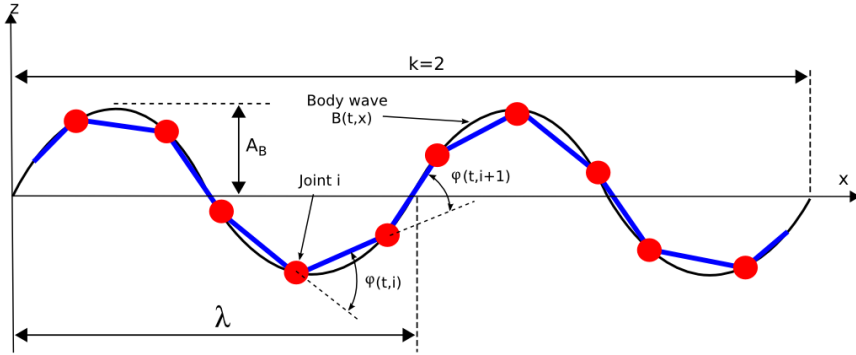


Fig. 3.6. A pitch-connecting modular robot at instant  $t$ , the body wave and its parameters.

For the  $H2$  subspace there appear two body waves:  $B_v(t, x)$  for the vertical joints and  $B_H(t, x)$  for the horizontal. Each wave has its own set of parameters  $A_B$ ,  $\lambda$  and  $k$ . The actual body wave  $B(t, x)$  is formed by the superposition of  $B_v(t, x)$  and  $B_H(t, x)$ .

## 4. Locomotion in 1D

### 4.1 Introduction

The locomotion of the pitch-connecting modular robots with  $M$  modules is studied based on the body waves that propagates throughout the robot. The solution space  $HI$  is used. Firstly the stability is analyzed and a condition for its achievement is proposed. Secondly a

relationship between the body wave and the step ( $\Delta x$ ) the robot perform during oneperiod is discussed. Then the minimal configuration is introduced. Finally, all the results are summarized as five locomotion principles.

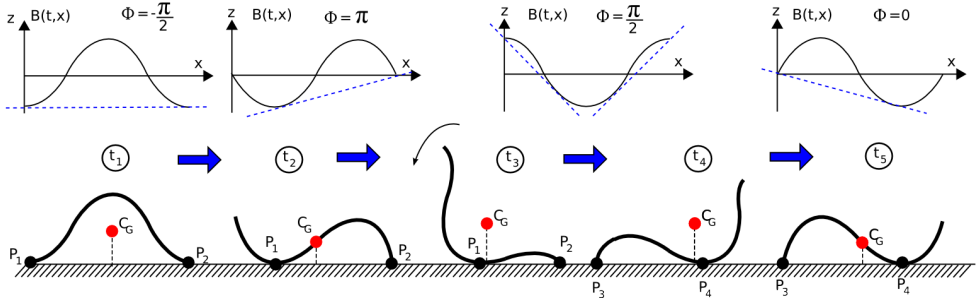


Fig 4.1. Stability of a pitch-connecting robot when its body wave have  $k=1$

#### 4.2 Stability condition

The robot is statically stable if for all  $t \in [0, T]$  the projection of the center of gravity fall inside the line that joins the two supporting points. This condition is only met when the  $k$  parameter is greater or equal to two. In addition, when this condition is satisfied, the height of the center of gravity remains constant all the time, making the gait very smooth. The explanation of this principle follows.

In figure 4.1 the body wave with  $k$  equals to one is shown at five different instants when the robot is moving during one period. The body wave phase  $\Phi$  at these chosen instants is  $-\pi/2$ ,  $-\pi$ ,  $\pi/2$ ,  $\pi/2 - \epsilon$  and  $0$ , where  $\pi/2 - \epsilon$  represents a phase quite close to  $\pi/2$  but smaller. The body wave is propagating to the right. The center of gravity is  $C_G$ . At  $t_1$  the two supporting points,  $P_1$  and  $P_2$  are located at the extremes of the robot. The projection of the center of gravity falls between the two. Therefore the robot is stable. During the transition between  $t_1$  and  $t_2$  the robot remains stable. The point  $P_1$  has moved to the right. During the transition from  $t_2$  to  $t_3$ , the system remains stable too. At  $t_3$  the projection of the center of gravity falls near  $P_1$  making the robot unstable. At this point,  $\Phi$  is  $\pi/2$ . At  $t_4$  the phase has decreased to  $\pi/2 - \epsilon$  making the projection of the center of gravity fall outside the  $P_1 P_2$  line. The robot pitch down to a new stable position in which the projection of the center of gravity fall again between the two new supporting points  $P_3$  and  $P_4$ . During the transition from  $t_4$  to  $t_5$  the robot remains stable.

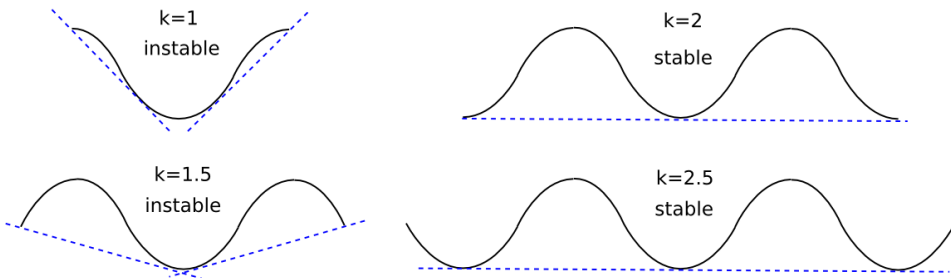
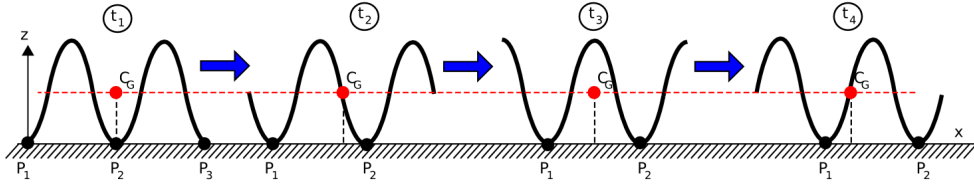


Fig 4.2. The body wave  $B(x,t)$  for different values of  $k$  when the phase is  $\pi/2$ Fig 4.3. Stability of a pitch-connecting robot when its body wave have  $k=2$ 

From the previous analysis it can be seen that the instability is because of the shape of the robot when the phase is near or equal to  $\pi/2$ . It is further analyzed in Fig. 4.2. A wave with a phase  $\pi/2$  is drawn for different points of the  $k$  parameter. When the value is greater or equal to two there are three or more points in contact with the ground. In these cases the system is stable.

In Fig 4.3 the motion of a pitch-connecting robot with  $k$  equal to two is shown. The projection of the center of gravity always falls in between the two supporting points. This type of motion is also very smooth due to the fact that the  $z$  coordinate of the center of gravity remains constant. It does not move up or down.

#### 4.3 Relationship between the robot step and the body wave

The step is the distance  $\Delta x$  along the  $x$  axis that the robot move in one period. The relationship between the step and the wavelength is given by the following equation:

$$\Delta x = \frac{L_T}{k} - \lambda \quad (13)$$

where  $L_T$  is the total length of the robot,  $\lambda$  is the wavelength and  $k$  the number of complete waves. It is only valid when the stability condition is met ( $k \geq 2$ ) and assuming that there is not any slippage on the points in contact with the ground.

In figure 4.4 a pitch-connecting robot with a body wave with  $k$  equals to two has been drawn at five different instants. The point  $P$  is the one that is in contact with the ground and where the condition of no slippage is applied. The  $L$  parameter is the length of the arc of one wave and it is equal to  $L_T/k$ . At instant  $t_i$ ,  $P$  is located at the left extreme of the robot. As the time increases, the body wave changes its phase and the point  $P$  moves to the right. When  $t=T$ ,  $P$  has moved a distance equal to  $L$ . The step can be calculated as the difference between the  $x$  coordinate of  $P$  at  $t_i$  and the  $x$  coordinate of point  $Q$  at  $t_f$ .  $Q$  is now the left extreme point of the robot:  $\Delta x = Q_x(t=T) - P_x(t=0) = P_x(t=T) - \lambda - P_x(t=0) = L - \lambda$

The equation (13) can be used to compare the motions caused by different body waves and is a criteria for choosing the ones that best fit a specific application. The body waves that have a high wavelength will perform a low step. Choosing a higher wavelength will let the robot to move a higher step.

The wavelength is also related to the amplitude  $A_B$ . A high amplitude means a low wavelength because of the total length of the robot is constant ( $L_T$ ). Therefore, a qualitative relation can be established between the amplitude and the step: the step grows with the increment in the amplitude. Robots using body waves with low  $A_B$  will perform a low step. On the contrary,

robots using high amplitudes will take high steps. Equation (13) will be used in future works to study deeply the kinematics of these robots.

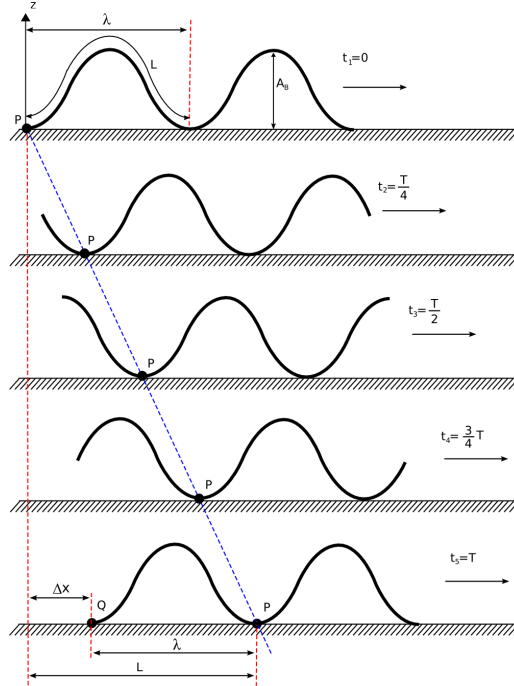


Fig 4.4. Relation between the step and the wavelength of a pitch-connecting robot when  $k=2$

#### 4.4 Minimal configuration

The relationship stated in section 4.3 is valid when the stability condition is met ( $k \geq 2$ ). As will be shown in section 4.5, the number of modules needed to satisfy that requirement is five. The group of the pitch-connecting robots with five or more modules is statically stable and the step can be calculated by means of equation (13).

When the number of modules is three or four, there cannot be two complete body waves moving along the robot. The  $k$  parameter is restricted to:  $0 < k < 2$ . Even if the statically stable movement can not be achieved, these robots can move. The stability is improved by means of lowering the amplitude  $A_B$ . This group has the property that at least one complete body wave can travel throughout the robot.

The last group comprised the robot which has only two modules. This robot is called a minimal configuration. It is the pitch-connecting robot with the minimum number of modules that is capable of moving in 1D. It is a new configuration that has not been previously studied by other researchers from the best of our knowledge. We have named it as pitch-pitch (PP) configuration.

In this configuration there is not any complete wave that traverse the robot ( $0 < k < 1$ ). But it can move. In addition the locomotion is statically stable. It always has at least two supporting points. The locomotion at five different instants it is shown in figure 4.5. A value of  $k=0.7$  ( $\Delta\phi=130$  degrees) is used. The gait starts at  $t_1$  by pitching down the joint 1. There appear a

small wave that propagates during the  $t_2$  to  $t_3$  transition. Then the joint 2 pitched up ( $t_4$ ) and the joint 1 start pitching down to complete the cycle. If the sign of the  $\Delta\Phi$  parameter is changed, the movement is performed in the opposite sense.

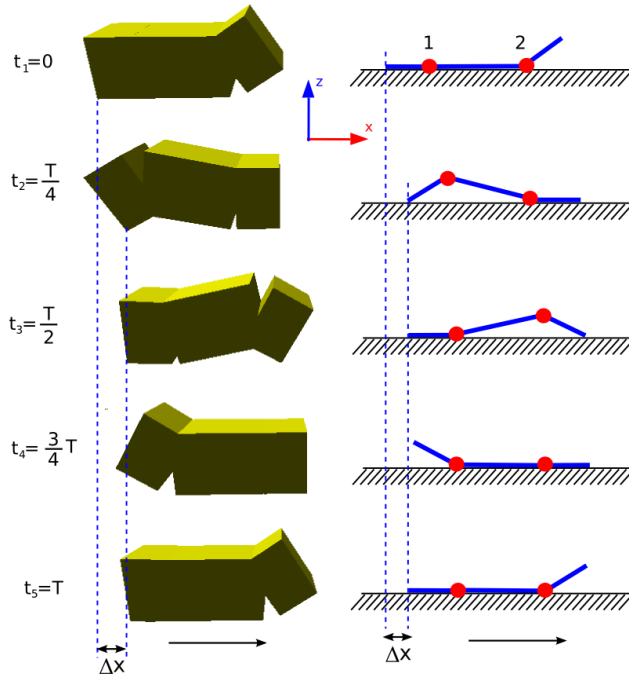


Fig. 4.5: Locomotion of the pitch-pitch (PP) minimal configuration.

The step of the robot ( $\Delta x$ ) is determined by the first movement from  $t_1$  to  $t_2$ . The rest of the time the mini-wave is propagated. As experiments show,  $\Delta x$  grows with the increase of the  $A$  parameter.

The minimal configurations are important for self-reconfigurable robot strategies. It gives us the maximum number of robot in which a bigger robot can be split. A self-reconfigurable robot with  $M$  modules can be split into a maximum of  $M/N$  smaller robots, where  $N$  is the number of modules of the minimal configuration.

#### 4.5 Locomotion principles

All the experimental results and the ideas introduced until now are summarized in five locomotion principles.

- *Locomotion principle 1*: The three parameters  $A$ ,  $\Delta\Phi$ , and  $T$  are enough to perform the locomotion of the pitch-connecting modular robots in 1D.

These parameters form the *H1* solution space. It is characterized by the appearance of body waves that traverse the robot. The period  $T$  is related to the velocity. The mean velocity during one period is:  $V = \Delta x / T$ . The  $\Delta\Phi$  parameter is related to the number of complete waves that appear (equation (6)). The  $A$  parameter is related to the amplitude of the body wave ( $A_B$ ) and to its wavelength ( $\lambda$ ).

- *Locomotion principle 2* : The locomotion of the pitch-connecting modular robots is because of the appearance of a body waves that traverse the robot. The sense of propagation of this wave determines if the robot moves forward or backward:
  - $\Delta\Phi < 0$ . The robot moves in one direction.
  - $\Delta\Phi > 0$ . The robot moves in the opposite direction.
  - $\Delta\Phi = 0, \Delta\Phi = \pi$ . There is not any traveling wave. There is no locomotion.
- *Locomotion principle 3* : The stability condition. The  $k$  parameter is related to the stability of the robot. For  $k \geq 2$  the locomotion is statically stable.

Using this principle the minimal number of modules needed to achieved statically stable locomotion can be calculated. Restricting the equation (6) to values of  $k$  greater or equal to two it follows that:  $k \geq 2 \Rightarrow \frac{M\Delta\Phi}{2\pi} \geq 2 \Rightarrow M \geq \frac{4\pi}{\Delta\Phi}$ . The number of modules is inversely proportional to  $\Delta\Phi$ .  $M$  is minimum when  $\Delta\Phi$  has its maximum value. For  $\Delta\Phi = 180$ ,  $M$  is equal to 4. But, from locomotion principle 2, when the phase difference is 180 degrees there is no locomotion. Therefore, the following condition is met:  $k \geq 2 \Rightarrow M \geq 5$ . In order to have a statically stable locomotion at least five modules are needed. In that situation the phase difference should satisfy:  $\Delta\Phi \geq \frac{4\pi}{5} \simeq 144$  degrees.

- *Locomotion principle 4*: The  $A$  parameter is related to the step ( $\Delta x$ ). The step increases with  $A$ .

As stated in section 4.3, the step ( $\Delta x$ ) increases with the amplitude of the body wave ( $A_B$ ). As will be shown in the experiments, the body wave amplitude also increases with the parameter  $A$ . Therefore, the step is increased with  $A$ .

- *Locomotion principle 5*: Only two modules are enough to perform locomotion in 1D. The family of pitch-connecting robots can be divided in three groups according to the number of modules they have:
  - Group 1:  $M=2$  Minimal configuration.  $k < 1$ . There is not a complete body wave.
  - Group 2:  $M \in [3, 4]$ .  $0 \leq k < 2$ . The Locomotion is not statically stable
  - Group 3:  $M \geq 5$ . Statically stable locomotion when  $k \geq 2$ .

## 5. Locomotion in 2D

### 5.1 Introduction

In this section the locomotion of the pitch-yaw-connecting modular robot with  $M$  modules is analyzed. The solutions are in the  $H2$  space. These robots can perform at least five different gaits: 1D sinusoidal, side winding, rotating, rolling and turnig. The locomotion in 1D have been previously studied. All the locomotion principles in 1D can be applied if the horizontal modules are fixed to its home position. In this case the robot can be seen as a pitch-connecting robot. The other gaits are performed in 2D. They will be analyzed in the following subsections and its principles can be derived of the properties of the body waves. The minimal configuration in 2D will be presented and finally all the ideas will be summarized in six locomotion principles.

### 5.2 Wave superposition

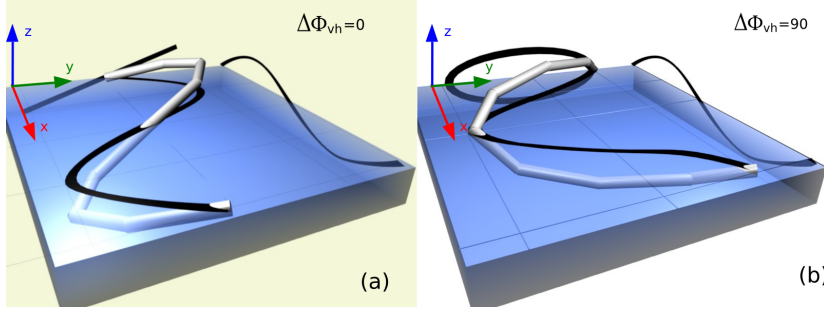


Fig 5.1. The body wave of the robot as a superposition of its horizontal and vertical body waves.

When working in the  $H2$  solution space there appear two body waves: one that propagates through the vertical modules ( $B_v(t, x)$ ) and another in the horizontal ones ( $B_h(t, x)$ ). Each having its own parameters:  $A_B$ ,  $\lambda$ , and  $k$ . The following properties are met:

1. The shape of the robot at any time is given by the superposition of the two waves:  $B(t, x) = B_v(t, x) + B_h(t, x)$ .
2. At every instant  $t$ , the projection of  $B(t, x)$  in the  $zy$ -plane is given by the phase difference between the two waves. In Fig.5.1 the shape of the robot is shown for two phase differences. In (a) the phase difference is 0. The projection in the  $zy$ -plane is a straight line. In (b) the phase difference is 90 degrees and the figure is an oval.
3. If the two waves propagate in the same direction along the  $x$  axis and with the same period  $T$  there appear a 3D wave that propagates in the same direction.

In the  $H2$  space, the period  $T$  is the same for the two waves. The property 3 is satisfied if the sign of the  $\Delta\Phi_v$  parameter is equal to the sign of  $\Delta\Phi_h$ . The condition for the appearance of a 3D traveling waves is:

$$\text{sign}(\Delta\Phi_v) = \text{sign}(\Delta\Phi_h) \quad (14)$$

The experiments show that the side winding and rotating gait is performed by the propagation of this 3D wave. If the equation (14) is not met the waves propagate in opposite directions and there is no locomotion. The movement is unstable and chaotic.

In addition, when that condition is satisfied the projection of  $B(t, x)$  remains constant over the time. Its shape is determined by the  $\Delta\Phi_{vh}$  parameter. This will be used in future work to study the stability and kinematics of the 2D gaits.

### 5.3 Side winding

The side winding gait is performed when the two body waves travel in the same direction (equation (14)) and with the same number of complete waves:

$$k_v = k_h \quad (15)$$

In Fig 5.2 a robot performing the side winding is shown, for  $k_v = k_h = 2$ .

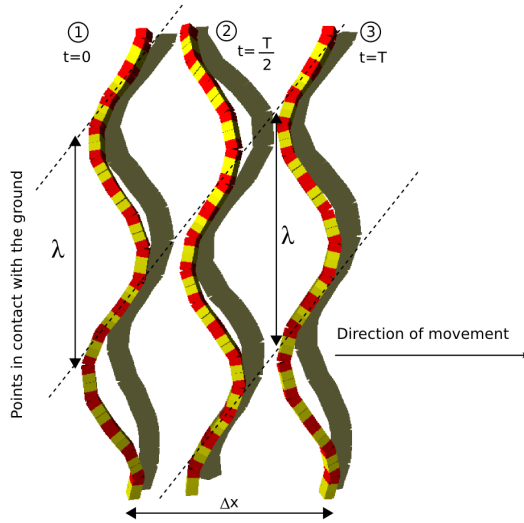


Fig 5.2. A pitch-yaw connecting robot performing the side winding gait with  $kv=kh=2$

The step after one period is  $\Delta x$ . There is a 3D body wave traveling through the robot. During its propagation some points are lifted and other are in contact with the ground. The dotted lines show the supporting points at every instant. They are in the same line. In the movement of the real snakes these lines can be seen as tracks in the sand.

Using the equation (6) the condition (15) implies that the parameters  $\Delta\Phi_v$  and  $\Delta\Phi_H$  should be the same. This is the condition for performing the side winding.

The parameter  $\Delta\Phi_{vH}$  determines the projection of the 3D wave in the  $zy$ -plane. When it is 0, as in the example of Fig. 5.1(a), all the modules are in the same plane. Therefore, all of them are in contact with the ground all the time. There is not any lifted point. In consequence the side winding is not performed. For values different from zero the shape is an oval, like in Fig. 5.1(b) and the gait can be realized.

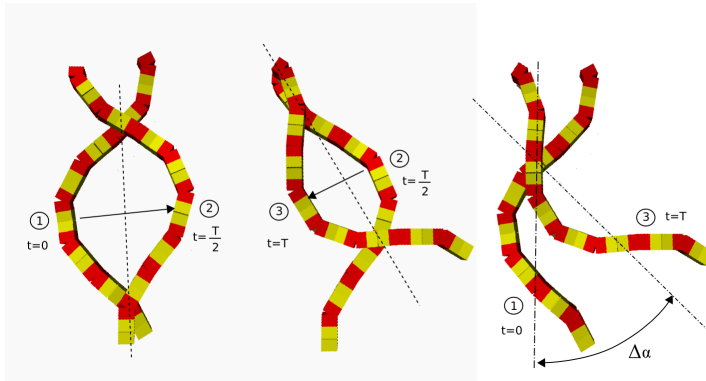


Fig. 5.3. A pitch-yaw connecting robot performing the rotating gait with  $kh=1$



The parameters  $A_h$  and  $A_v$  are related to the radius of the oval of the figure in the  $yz$ -plane. Experiments show that smooth movements are performed when the  $A_h/A_v$  is 5 and the values of  $A_h$  are between 20 and 40 degrees. The stability and properties of this movement depend on the  $zy$ -figure and a detailed analysis will be done in future work.

#### 5.4 Rotating

The rotating gait is a new locomotion gait not previously mentioned by other researchers from the best of our knowledge. The robot is able to yaw, changing the orientation of its body axis. It is performed by means of two waves traveling in the same direction. The condition that should be satisfied is the following:

$$k_v = 2k_h \quad (15)$$

Using equation (6), this condition can be rewritten as:  $\Delta\Phi_v = 2\Delta\Phi_h$ .

In figure 5.3 this gait is shown at three different instant for  $k_h=1$ . The movement starts at  $t=0$ . As the 3D body wave propagates the shape changes. At  $T/2$  the new shape is a reflection of the one at 0. Then the waves continuous its propagation and the robot perform another reflection. After these two reflections the robot has rotated  $\Delta\alpha$  degrees. In the right part of Fig. 5.3 the final rotation  $\Delta\alpha$  is shown. The actual movement is not a pure rotation but rather a superposition of a rotation and a displacement. But the displacement is very small compared to the rotation. The experiments show that the value of the  $\Delta\Phi_{vh}$  can be in the range  $[-90, 90]$  and that the  $A_h/A_v$  ratio should be in the range  $[8, 10]$  for a smooth movement.

#### 5.5 Rolling

Pitch-yaw connecting modular robots can roll around their body axis. This gait is performed without any traveling wave. The parameters  $\Delta\Phi_v$  and  $\Delta\Phi_h$  should be zero and  $\Delta\Phi_{vh}$  equal to 90 degrees. The two amplitudes  $A_v$  and  $A_h$  should be the same. The rolling angle is 360 per period. In figure 5.4 the rolling gait is being performed by a 16 modules pitch-yaw-connecting robots. The movement is shown at 3 instants. After  $T/4$  the robot has rolled 90 degrees. The direction of movement is controlled by the sign of  $\Delta\Phi_{vh}$ .

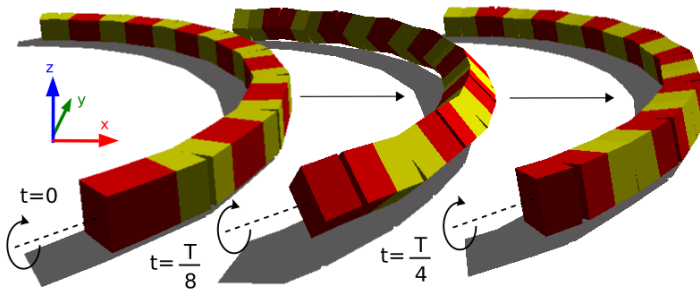


Fig. 5.4. A pitch-yaw connecting robot performing the rolling gait

### 5.6 Turning gait

Pitch-yaw connecting modular robot can move along a circular arc for turning left or right. There is only one traveling wave along the vertical modules. The horizontal joints are fixed to an angle  $O_H$  different from 0.  $O_H$  is used to determine the shape of the robot during the turning. It can be calculated using the equation (16), where  $\Delta S$  is the length of the arc in degrees and  $M$  the total modules of the robot.

$$O_H = \frac{\Delta S}{M/2} \quad (16)$$

if  $\Delta S$  is equal to  $2\pi$  the robot has the shape of a polygon and perform a rotation around its center. The experiments show that the  $k$  parameter should be big enough to guarantee the stability of the robot. In Fig. 5.5 the robot is turning right for  $k=3$  and  $M=16$ .

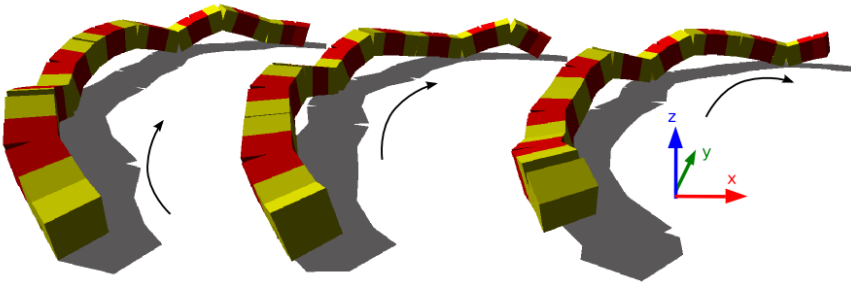


Fig. 5.5. A pitch-yaw connecting modular robot performing the turning gait for  $k=3$ .

### 5.7 Minimal configurations

The minimal configuration is the robot with the minimal amount of modules that is able to perform locomotion in 2D. It has been found that this minimal configuration consist of three modules ( $M=3$ ). It is a new configuration not previously studied by other researchers. We call it pitch-yaw-pitch configuration (PYP). It composed by two pitch modules at the extremes and a yaw module in the center. It can perform five gaits: 1D sinusoidal, turning, rolling, rotating and lateral shifting.

There is not any horizontal body wave as there is only one horizontal module. Therefore the parameter  $\Delta\Phi_H$  is not needed. The rest of the parameters used are:  $A_v$ ,  $A_h$ ,  $\Delta\Phi_v$ ,  $\Delta\Phi_{vH}$ ,  $T$  and  $O_h$ .

The pitch-yaw-pitch configuration can move in 1D forward and backward. The coordination is exactly the same as the one for the pitch-pitch configuration. The module in the middle is set up with an offset equal to 0 ( $O_h=0$ ). The movement is performed as was shown in figure 4.5. If the offset  $O_h$  is set to a value different from zero the robot describes a circular arc.

The rolling gait is shown in Fig. 5.6. This gait is performed when the two amplitudes are the same and their values bigger than 60 degrees. The two vertical modules are in phase ( $\Delta\Phi_v=0$ ) and the horizontal is 90 degrees out of phase ( $\Delta\Phi_{vH}=90$ ). Initially it has the shape of the ">" symbol. The vertical modules start to pitch down while the middle module yaws to its home position. At  $T/4$  the robot has rolled  $\pi/2$ . The orientation of the modules has changed:

pitching modules have become yawing ones and vice-versa. Then the module in the middle pitch up while the others move to their home positions. At  $T/2$  the robot has its initial “>” shape. It has rolled 180 degrees and moved a distance  $\Delta x$  along the x axis, perpendicular to its body axis.

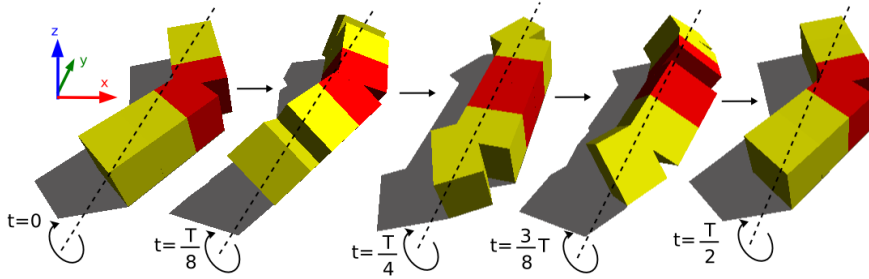


Fig. 5.6. The minimal configuration pitchyaw-pitch (PYP) performing the rolling gait

The lateral shift gait is shown in Fig. 5.7(b). The parameters have the same value than in the rolling case, but the amplitudes should have a value less than 40. The extreme modules perform a circular movement. They are in contact with the ground from instants  $t_3$  to  $t_5$ . The yaw module is lifted and moved to a new position.

The rotating gait is shown in Fig. 5.7(a). The parameter  $\Delta\Phi_{VH}$  and  $\Delta\Phi_V$  are 90 and 180 degrees respectively.

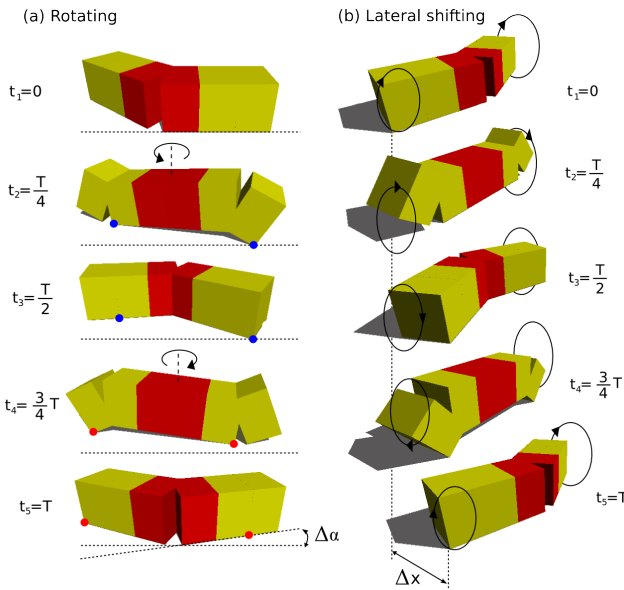


Fig. 5.7. The pitch-yaw-pitch minimal configuration performing the (a) Rotating gait. (b) Lateral shifting.

This movement is completed in two stages. From  $t_1$  to  $t_3$  the yawing module move to the back changing from the ">" shape to a "<". From  $t_3$  to  $t_5$  the yawing module is moved to the forth to its initial ">" shape. The robot perform the same two reflections than in the general case. During the reflection the pitching modules have different points in contact with the ground. It makes the robot to perform a rotation of  $\Delta\alpha$ .

In table 5.1 all the relationships between the parameters for achieving the rolling, rotating and shifting gaits are summarized.

PYP parameters	Rolling	Rotating	Lateral shifting
$A_v$	$A_v = A_h > 60$	0-90	$A_v < 40$
$A_h$	$A_v = A_h > 60$	0-90	$A_h < 40$
$O_h$	0	0	0
$\Delta\Phi_v$	0	180	0
$\Delta\Phi_{vH}$	90	90	90

Table 5.1: The PYP parameters and their values for achieving the rolling, rotating and lateral shifting gaits.

### 5.8 Locomotion principles

All the experimental results and the ideas introduced in this section are summarized in five locomotion principles:

- Locomotion principle 6: Seven parameters are needed to perform locomotion in 2D:  $A_v$ ,  $A_h$ ,  $\Delta\Phi_v$ ,  $\Delta\Phi_h$ ,  $\Delta\Phi_{vH}$ ,  $O_h$  and  $T$ . At least four 2D gaits can be achieved: side winding, rotating, rolling and turning.

The solutions are in the  $H2$  space and are characterized by the appearance of two body waves for both, the vertical and the horizontal modules.

- Locomotion principle 7: the two waves should propagates in the same direction. A 3D wave appear on the robot that propagates along its body axis. Its projection on zy-plane is a fixed figure. It should be satisfied that  $sign(\Delta\Phi_v) = sign(\Delta\Phi_h)$ . The sign determines the sense of propagation of the 3D wave along the x axis: forward or backward.
- Locomotion principle 8: The side winding gait is characterized by two waves travelling in the same direction and with the same  $k$  parameter. The condition that should be met is:  $\Delta\Phi_v = \Delta\Phi_h$ . If the sense of propagation of the 3D wave is changed the motion is perform in the opposite sense.
- Locomotion principle 9: The rotating gait is characterized by two waves that propagates in the same direction with  $k_v$  parameter double than  $k_h$ . The condition that should be met is  $\Delta\Phi_v = 2 \Delta\Phi_h$ . The direction of propagation of the 3D wave determines if the rotating is clock-wise or counterclockwise.
- Locomotion principle 10: Rolling gait is characterized by no traveling waves:  $\Delta\Phi_v = \Delta\Phi_h = 0$ . The parameter  $\Delta\Phi_{vH}$  should be 90 and  $A_v = A_h$ .
- Locomotion principle 11: Circular turning is characterized by one travelling wave along the vertical modules and no wave on the horizontal.  $\Delta\Phi_h = 0$ . The  $O_h$  parameter determines the shape of the robot when turning.

- Locomotion principle 12: Only three modules are enough to perform the four locomotion gaits in 2D.

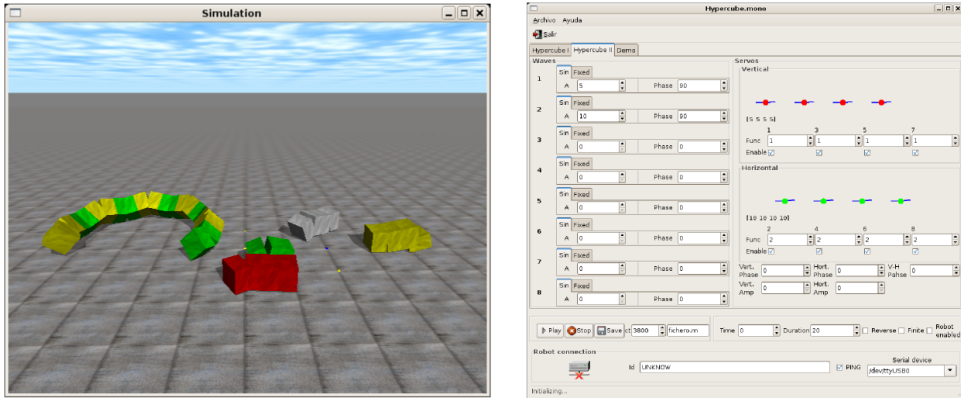


Fig 6.1. The software environment developed. Left: The physical simulator. Right: robot control interface.

## 6. Experiments

All the locomotion principles has been obtained by means of simulations. Then they have been tested on real modular robots prototypes. In this section the software and the robot prototypes are briefly introduced and the results of the experiments are discussed.

### 6.1 Software

A software application has been developed to both simulate the modular robots and control the real robots prototypes. Two screenshots are shown in Fig. 6.1. The applications have been written in C and C# languages and they run in Linux systems. The simulator is based on the Open Dynamics Engine (ODE) to perform the physical simulations. An Application Programming Interface (API) has been design to easily build and test 1D topology modular robots. All the data generated during the simulations can be dump into a Matlab/Octave file for processing and drawing.

The second application is a robot control software for moving the real prototypes. It consist of a graphical interface that let the user to set up all the parameters of the sinusoidal generators. The bending angles ( $\varphi, f$ ) are sent to the robot through a serial link.

### 6.2 Modular Robots prototypes

Four modular robots prototypes have been built to test the locomotion principles. They all are based on the Y1 modules (Fig. 6.2(a)). These are a very cheap and easy to build modules. They only have one degree of freedom actuated by an RC servo. The rotation range is 180 degrees.

The two minimal configurations are shown in Fig. 6.2(b). They consist of two and three modules respectively. Two eight modules robots have been built. One is a pitch-connecting modular robot (Fig. 6.2(c)) and the other a pitch-yaw one (Fig. 6.2(d)).

All the prototypes have the electronic and power supply outside. The electronic consist of an 8-bit microcontroller (PIC16F876A) that generates the Pulse Width Modulation (PWM) signals to command the servos. The robots are connected to a PC by a serial link.

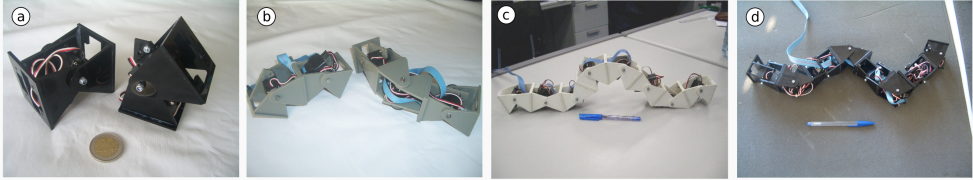


Fig 6.2. The four robot prototypes built. (a) The Y1 modules used to built the robot. (b) The two minimal configurations: PP and PYP. (c) An eight modules pitch-connecting modular robot . (d) An eight modules pitch-yaw-connecting modular robot.

### 6.3 Simulation results for locomotion in 1D

The experimental results shown have been obtained for a modular robot of 8 pitch-connecting modules moving in 1D along the  $x$  axis. The amplitude( $A$ ) used is 45. The module four is taken as a reference. All the graphs show the coordinates and rotation angles of this module. In Fig. 6.3(a) the evolution of the  $x$ -coordinate is shown for  $k=2$  (stability condition). It can be seen that it is quite similar to a uniform rectilinear movement. The sign of the  $\Delta\Phi$  parameter determine the slope of the graph. Changing its signs makes the robot move the in the opposite direction.

In figure 6.3(b) the step along the  $x$  axis versus the phase difference is shown. When  $\Delta\Phi$  is 0, 180 or -180 no step is given ( $\Delta x=0$ ), as stated by the locomotion principle 2. For values between -50 and 50 the movement is far from the stability condition and the step oscillates with  $\Delta\Phi$ . It is a region that should be avoided.

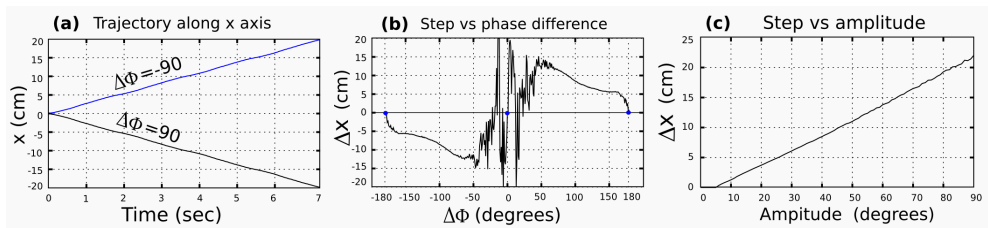


Fig. 6.3. Experiments for the Locomotion in 1D of an 8 modules pitch-connecting modular robot.

The step versus the amplitude ( $A$ ) is shown in Fig. 6.3(c). The more amplitude the more step, as stated by the locomotion principle 4. The relationship is very close to be linear.

The experiments for the stability condition are shown in Fig. 6.4. The trajectory and the pitching angle of the reference module are drawn for different values of the  $k$  parameter. When  $k$  is less than two the trajectory is not uniform. There are instants where the  $x$

coordinate decreases with time. The pitching angle is not uniform too. There are some peaks in which it changes abruptly. When the  $k$  is equal or greater than two (stability condition) both the trajectory and the pitching angle are smooth and there is not any instability in the locomotion, as stated by the locomotion principle 3.

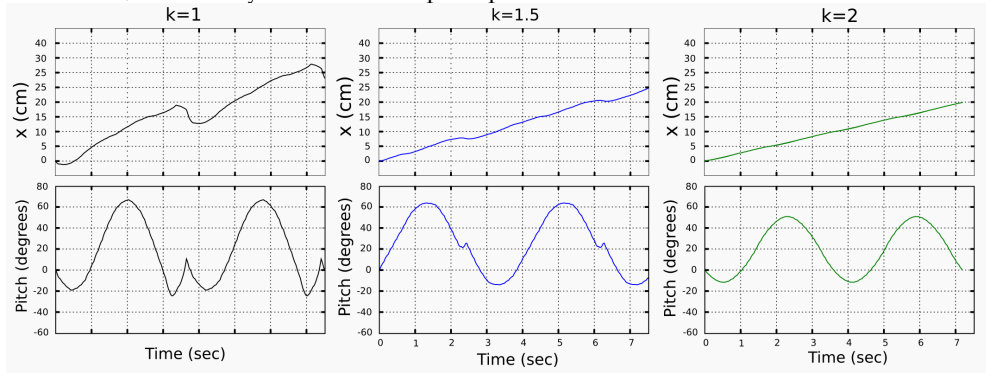


Fig. 6.4. Stability condition experiments for the pitch-connecting modular robot.

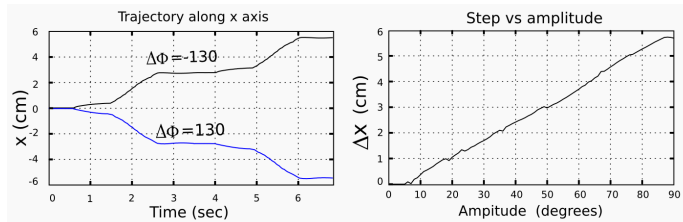


Fig. 6.5. Experiments for the locomotion of the pitch-pitch minimal configuration

The simulation results for the minimal pitch-pitch (PP) configuration are shown in figure 6.5. The trajectory along  $x$  axis for two periods is shown in the left. The locomotion is not uniform. There are regions where the robot remains stopped and other where it is moving. When the sign of  $\Delta\Phi$  is changed the direction of the movement is performed in the opposite direction. The step also increases with the amplitude, as can be seen in the right.

#### 6.4 Simulation results for locomotion in 2D.

The experimental results shown have been obtained for an eight modules pitch-yaw-connecting modular robot. The module four has been used as a reference. Its coordinates  $x, y$  and yawing angles are shown in the graphics.

The results for the side winding gait are shown in figure 6.6(a). The  $y$  coordinate is shown in the upper picture for the traveling 3D wave moving in two senses of direction. After two periods the  $y$  position has increased (decreased) nearly 30 cm. In the lower picture the yawing angle is shown. It can be seen that after the two periods the yawing angle has changed  $\Delta\alpha$ . The side winding has also a small rotation that is superpose to the lateral movement.

The rotating gait is shown in Fig. 6.6(b). Both the  $x$  and  $y$  coordinates are changing. After two periods the yawing angle is 40 (-40) degrees. When the sense of propagation of the 3D wave is changed, the movement is performed in the opposite sense.

The experimental results for the rolling gait are shown in Fig. 6.6(c). The movement along the  $y$  axis is very uniform and the angular velocity of the rolling gait remains constant.

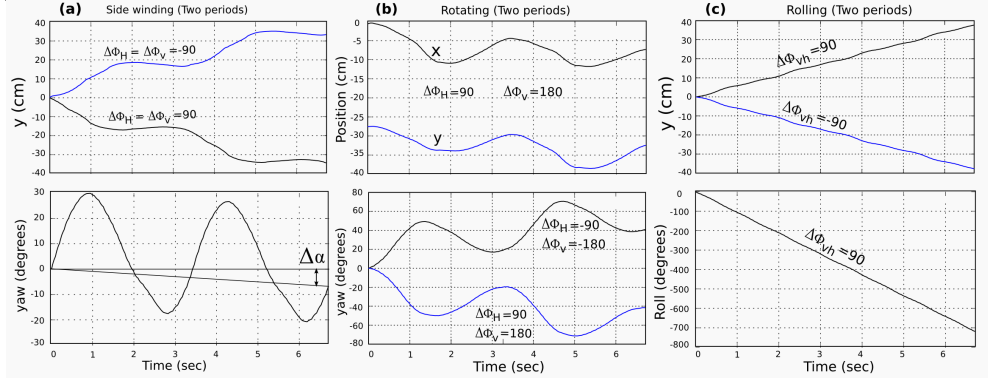


Fig. 6.6. Experimental results for the side winding, rotating and rolling gaits.

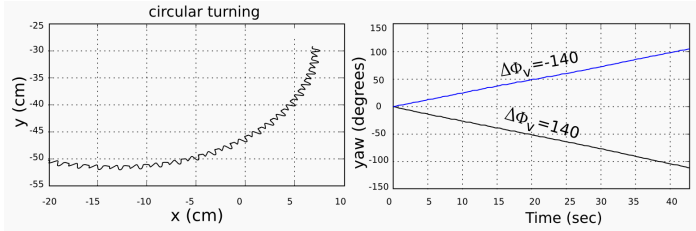


Fig. 6.7. Experimental results for the turning gait

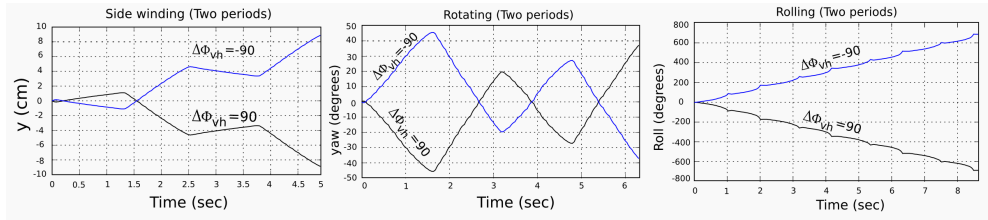


Fig 6.8. Experimental results for the pitch-yaw-pitch (PYP) minimal configuration.

The turning gaits results are shown in Fig. 6.7. The trajectory of the robot is a circular arc and the yawing angle is constant.

Finally, the experimental results for the pitch-yaw-pitch minimal configuration are shown in Fig. 6.8. In general, the  $x, y$ , yaw and roll variations are not as smooth as in the eight modules cases.

## 7. Conclusions

The Locomotion principles for the groups of pitch and pitch-yaw-connecting modular robots have been studied, simulated and finally tested on real robots. Five different gaits have been



achieved: 1D sinusoidal, rolling, rotating, turning and side winding. The rotating gait is a new one not previously mentioned by another researchers from the best of our knowledge. All the gaits have been implemented using a biologically inspired model based on sinusoidal generators that can be implemented efficiently on low cost microcontrollers.

The minimal configurations for both locomotion in 1D and 2D have been found. They are novel configurations that minimize the number of modules and therefore maximize the number of robots in which a self-reconfigurable robot can split into.

Finally a complete new simulation environment for 1D topologies robots has been developed and used to collect all the data needed for the study of the locomotion principles.

## 8. Future works

In future works the relationships between the sinusoidal generator parameters and the kinematics will be further studied. Also, the kinematics of the 2D gaits will be developed based on the shape of the 3D waves. The climbing properties of the pitch-yaw-connecting modular robots will be analyzed. Another research line is the study of the 2D topologies.

## 9. References

- Castano, A.; & Shen, W.M. (2000). CONRO: Towards Miniature Self-Sufficient Metamorphic Robots, *Autonomous Robots*, Vol.13, 2000, pp.309-324.
- Chen, L.; Wang, Y. & Ma, S. (2004) Studies on Lateral Rolling Locomotion of a Snake Robot, *Proceeding of IROS2004* pp. 5070-5074, Sendai, Japan, Sept., 2004.
- Chen, W.M.; Krivokon, M.; Chiu, H.; Everist, J. & Rubenstein, M. (2006). Multimode Locomotion via SuperBot Reconfigurable Robots. *Autonomous Robots*, Vol.20, 2006, pp.165-177
- Conradt J. & Varshavskaya P (2003), *Distributed central pattern generator control for a serpentine robot*. ICANN 2003.
- Crespi, A.; Badertscher, A.; Guignard, A. & Ijspeert A.J. (2005). Swimming and Crawling with an Amphibious Snake Robot. *Proc. IEEE. Int. Conf. on Robotics and Automation*, pp. 3024- 3028, 2005.
- Granosik, G.; Hansen, M. G. & Borenstein, J. (2005). The Omnitread Serpentine Robot for Industrial Inspection and Surveillance, *Industrial Robot: An International Journal*, Vol.32, No.2, 2005, pp.139-148.
- Gonzalez-Gomez J.; Aguayo, E; & Boemo, E. (2004). Locomotion of a Modular Worm-like Robot using a FPGA-based embedded MicroBlaze Soft-processor. *Proceeding of the 7th International Conference on Climbing and Walking Robots, CLAWAR 2004*, pp. 869-878, Madrid, Spain, September, 2004.
- Gonzalez-Gomez, J. & Boemo E., (2005). Motion of Minimal Configurations of a Modular Robot: Sinusoidal, Lateral Rolling and Lateral Shift, *Proceeding of the 8th International Conference on Climbing and Walking Robots, CLAWAR 2005*, pp. 667-674, London, U.K., September, 2005.
- Gonzalez-Gomez, J.; H. Zhang, Boemo, E. & Zhang, J. (2006). "Locomotion Capabilities of a Modular Robot with Eight Pitch-Yaw-Connecting Modules", *The 9th International*

- Conference on Climbing and Walking Robots, CLAWAR2006*, pp. 150-157, Brussels, Belgium, September, 2006.
- Hirose, S. & Morishima, A. (1990). Design and control of a mobile robot with an articulated body, *The International Journal of Robotics Research*, Vol. 9 No. 2, 1990, pp. 99-113.
- Hirose, S. (1993). *Biologically inspired robots (snake-like locomotor and manipulator)*, Oxford University Press, 1993.
- Klaassen, B. & Paap, K.L. (1999). GMD-SNAKE2: a snake-like robot driven by wheels and a method for motion control, *Proceedings of IEEE International Conference on Robotics and Automation*, pp. 3014-3019, Detroit, MI, 10-15 May, 1999.
- Kurokawa, H.; Kamimura, A.; Yoshida, E.; Tomita, K. & Kokaji, S. (2003). M-TRAN II: Metamorphosis from a Four-Legged Walker to a Caterpillar. *Proceedings of the 2003 IEEE/RSJ Intl. Conference on Intelligent Robots and Systems*, pp. 2454-2459, October 2003.
- Ma S.; & Tadokoro N. (2006). Analysis of Creeping Locomotion of a Snake-like Robot on a Slope. *Autonomous Robots*, Vol. 20, Issue 1, Jan 2006, pp. 15 - 23.
- Miller, P.G. (2002). Snake robots for search and rescue. *Neurotechnology for Biomimetic Robots*. 2002, MIT Press, pp. 271-284.
- Moechel, R.; Jaquier, C.; Drapel K., Dittrich E. & Upegui A. (2005). Yamor and Bluemove-an Autonomous Modular Robot with Bluetooth Interface for Exploring Adaptive Locomotion, *Proceeding of the 8th International Conference on Climbing and Walking Robots, CLAWAR 2005*, pp. 685-692, London, U.K., September 2005.
- Mori, M. & Hirose, S. (2002). "Three-dimensional Serpentine Motion and Lateral Rolling by Active Cord Mechanism", *Proceeding of the 2002 IEEE/RSJ International Conference on Intelligent Robots and Systems*, pp.829-834, Lausanne, Switzerland, Oct. 2002.
- Ute, J. & Ono, K. (2002). Fast and efficient locomotion of a snake robot based on self-excitation principle. *Proceeding of the 7th International Workshop on Advanced Motion Control*, pp. 532- 539, 2002.
- Yamakita M.; Hashimoto, M. & Yamada, T. (2003), Control of Locomotion and Head Configuration of 3D Snake Robot. *Proceedings of the 2003 IEEE International Conference on Robotics & Automation*, pp. 2055-2060, September 2003.
- Yim, M. & David, G. (2000). PolyBot: a Module Reconfigurable Robot, *Proceedings of the 2000 IEEE International Conference on Robotics and Automation*, pp.514-520, San Francisco, CA, USA, April, 2000.
- Yim, M.; Roufas, K.; Duff, D.; Zhang, Y.; Eldershaw, C. & Homans, S. (2003), Module Reconfigurable Robot in Space Application, *Autonomous Robots*, Vol. 14, Issue 2-3, 2003, pp.225-237.
- Zhang, H.; Wang W.; Deng, Z. & Zong, G. (2006a): A Novel Reconfigurable Robot for Urban Search and Rescue, *International Journal of Advanced Robotic Systems*, Vol.3 No.4, 2006, pp.359-366.
- Zhang, H.; Deng, Z.; Wang, W.; Zhang, J. & Zong, G. (2006b). Locomotion Capabilities of a Novel Reconfigurable Robot with 3 DOF Active Joints for Rugged Terrain, *Proceedings of the 2006 IEEE/RSJ International Conference on Intelligent Robots and Systems, IROS 2006*, pp.5588-5593, Beijing, China, October, 2006
- Zong, G.; Deng, Z.; & Wang, W. (2006) Realization of a Modular Reconfigurable Robot for Rough Terrain, *Proceedings of the 2006 IEEE International Conference on Mechatronics and Automation*, pp. 289-294, Luoyang, Henan, China, June, 2006.